THE EFFECT OF RARE EARTH Dy^{3+} IONS ON STRUCTURAL, DIELECTRIC AND ELECTRICAL BEHAVIOR OF $Ni_{0.4}Co_{0.6}Dy_yFe_{2-y}O_4$ NANO-FERRITES SYNTHESIZED BY WET CHEMICAL APPROACH

M. F. ALY ABOUD[a,b*], I. AHMAD[c], S. ARSHAD[c], S. LIAQAT[d], Z. A. GILANI[e], Q. NADEEM[d], I. SHAKIR[a]

[a]Sustainable Energy Technologies (SET) center, College of Engineering, King Saud University,PO-BOX 800, Riyadh 11421, Kingdom of Saudi Arabia
[b]Mining, Metallurgical and Petroleum Engineering Department, Faculty of Engineering,Al-Azhar University, Nasr City, Cairo 11371, Egypt
[c]Department of Chemistry, Allama Iqbal Open University, Islamabad 44000,Pakistan
[d]Department of Chemistry, The Islamia University of Bahawalpur, Bahawalpur-63100, Pakistan
[e]Department of Physics, Balochistan University of Information Technology, Engineering and Management Sciences (BUITEMS) , Quetta 87300, Pakistan

Cobalt nickel nanoferrites doped with dysprosium with nominal composition $Ni_{0.4}Co_{0.6}Dy_yFe_{2-y}O_4$ (where y = 0.0, 0.03, 0.06, 0.09, 0.12 and 0.15) were prepared by micro-emulsion method. The annealing temperature was determined from thermogravimetric analysis (TGA) data. X-ray diffraction (XRD) studies showed a prominent 311 peak which is a characteristic of simple spinel phase and is strong evidence of face centered cubic structure. X-ray studies also demonstrated that these ferrites have crystallite sizes in the range of 25-40 nm. Fourier transform infrared (FTIR) studies confirmed the presence of Dy^{3+} in place of Fe^{3+} in these ferrites. Two prominent peaks were appeared in the octahedral range of 350-500 cm^{-1} in FTIR spectra. Dielectric studies revealed the significant decrease in dielectric constant and other dielectric parameters with the increased Dy^{3+} ions. The materials with minimum dielectric loss are required for high frequency devices fabrication. DC-electrical resistivity was also recorded at varied temperature in the range of 298 to 572 K.$Ni_{0.4}Co_{0.6}Fe_2O_4$ exhibited the DC resistivity 6.30×10^8 Ωcm while significant increase (~10 %) in this value (6.90×10^8 Ωcm) was observed for $Ni_{0.4}Co_{0.6}Dy_{0.15}Fe_{1.85}O_4$ nano-ferrites.

1. Introduction

Nanoparticles that have usually diameter in the range of 1-100 nm have several extraordinary features absolutely different from their bulk counter parts. Nanomaterials separately exist in the form of particles, crystals, nanowires, nanotubes and quantum dots. In collective form they exist as arrays, assemblies and super lattices[1, 2] . Nanoparticles containing iron particles are known as nano-ferrites. They may also contain other metals such as cobalt, nickel, dysprosium, zinc and magnesium etc. These metals impart various fantastic properties to ferrites which are greatly affected by changing proportions of metals. The properties of nanoparticles deviate from the bulk material. This deviation of properties is due to the surface to volume ratio as well as size of the particles. Small particle size is preferred over large size due to novel electrical and magnetic properties of nanoparticles compared to the bulk material[3] . Particles interaction and their chemical composition also affect their properties. When their surface to volume ratio increases, the

_____
*Corresponding author: maboud@ksu.edu.sa

behavior and properties of atoms which are on the surface of particles dominate on the behavior and properties of atoms which are in the interior part of particles. This dominance of surface atoms on the interior ones is due to the fact that surface atoms have less coordination number than interior atoms due to variation in geometry[4].

Ferrites are vital magnetic materials with high resistivity for a variety of modern advanced electronic devices fabrication[5]. Spinel ferrites are intensely focused in research due to their exclusive crystal structure and microstructure[6, 7] .

Due to their unique features, ferrites are playing major role in different fields e.g., they are used in the fabrication of high quality filters around the cables as ferrite rings due to their excellent property of rapid response towards oscillating field. Further, ferrite material with high DC electrical resistivity is used in high frequency devices. Due to ferromagnetic nature, ferrite material is also used in the fabrication of magnetic semiconductors. Apart from these, they are also employed in several other fields such as, microwave , radio wave, computer, telecommunication and several other technologies[8-10].

One of their interesting features is that their properties can be changed by controlling and changing the concentration of metals used. Spinel soft ferrites contain metals like cobalt, nickel, zinc and magnesium apart from iron. Cobalt metal can alter the electrical resistivity and activation energy. Nickel metal controls the dielectric properties of spinel ferrites[8] . Dysprosium have 4f electrons which play a major role in originating magnetic anisotropy due to their orbital shape and also have effect on electrical properties by increasing electrical resistivity[11]. Other salient features of the nano-ferrites material are conductivity and magnetism which are due to the spin coupling mechanism. Coupling takes place between 3d electrons by Fe-Fe interaction. These properties can also be changed by the doping of some rare earth metal in these ferrites. This leads to the 3d-4f coupling due to interaction of Fe-RE (rare earth).This variation in properties is due to the presence of unpaired electrons in the 4f orbital of rare earth metal .

A lot of methods have been reported for the synthesis of nano-ferrites such as micro-emulsion[8] , sol-gel[12], co-precipitation[13], citrate precursor[14], microwave assisted hydrothermal [15] and reverse micelle[16] . Among all these methods micro-emulsion method has been proved excellent and reproducible in which nanoparticles with controllable size and narrow size distribution can be obtained. In this method, an emulsion is formed when a surfactant is mechanically agitated with the oil and water which results in the formation of two phase dispersion in which one phase is in the form of droplet coated with surfactant and is dispersed in the other phase in continuous manner. Here surfactant controls the particle size which in turn controls the electrical and magnetic properties.

In present study we have used micro-emulsion method to fabricate the resistive dysprosium substituted nickel cobalt nano-ferrites for high frequency device applications.

2. Experimental work

2.1.Synthesis route

Dysprosium substituted nickel cobalt nanoferrites $Ni_{0.4}Co_{0.6}Dy_yFe_{2-y}O_4$ (y = 0.0, 0.03, 0.06, 0.09, 0.12 and 0.15) were synthesized by micro-emulsion method[17]. Cetyltrimethylammonium bromide (CTAB) was used as a surfactant which is an emulsifying agent. Aqueous solutions following metal salts of required molarity were prepared in deionised water: nickel (II) nitrate hexahydrate (97%) $Ni(NO_3)_2.6H_2O$, cobalt (II) nitrate hexahydrate (>98 %) $Co(NO_3)_2.6H_2O$, iron (III) nitrate nonahydrate (>98 %) $Fe(NO_3)_3.9H_2O$, dysprosium nitrate hydrate (99.9%) $Dy(NO_3)_3.xH_2O$. All these solutions were mixed in stoichiometric ratio in six different beakers (each corresponds to a specific composition). The temperature of all reaction mixtures was raised to about 50-60 ^{o}C. Equal volume of CTAB aqueous solution was added to each reaction mixture. pH of these solutions was elevated to 10-11 by adding aqueous ammonia (2M) drop wise. Ammonia solution contains OH^- ions and these ions react with metal ions present in the solution to form hydroxide of metals in the form of precipitates. All the reaction mixtures were covered by aluminium foil to avoid evaporation of ammonia and further 4-5 hrs stirring was carried out at room temperature to ensure the complete precipitation. Precipitates were filtered and

washed with deionised water to remove all the water soluble impurities. The drying of all samples was done overnight at about 100 $^{\circ}$C. After grinding the precipitates, the annealing was carried out for 6 hrs.

2.2.Characterization techniques

Samples prepared were characterized by TGA, XRD, FTIR, DC electrical resistivity and dielectric measurements. TGA was done by SDT 2960 TGA instrument to know the annealing temperature which was required for the preparation of spinel phase. XRD patterns were recorded on Philips X'Pert PRO 3040/60 diffractometer with a radiation source of Cu K$_\alpha$ with wavelength 1.54 Å. Structure and crystallite size was calculated from XRD. Perkin Elmer FTIR spectrum-2000 spectrometer was used for recording FTIR spectra. Dielectric measurements were performed by E4991A RF Impedance / Material analyzer. DC electrical resistivity measurements were performed by two point probe method by employing Kiethly-2400 source meter.

3. Results and discussion

3.1.Thermogravimetric analysis (TGA)

The thermogram of un-annealed sample of ($Ni_{0.4}Co_{0.6}Fe_2O_4$) is shown in the Figure 1. According to this thermogram the weight loss occurred in various stages. The first stage shows the desorption of adsorbed water in the samples. Second stage is due to weight loss when conversion of hydroxides to the oxides of ferrite sample take place. The third and last stage is attributed to the formation of spinel structure. The similar thermogravimetric results have been reported by our group for ferrite and perovskite nanoparticles [18, 19].
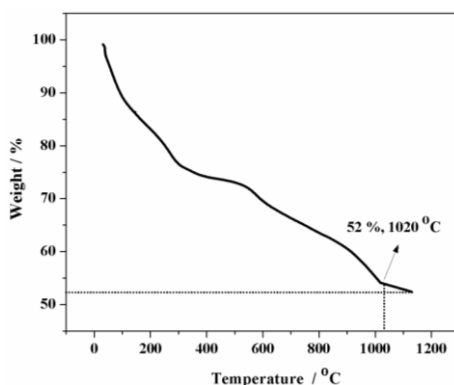

Fig.1. TGA of un-annealed sample of Ni$_{0.4}$Co$_{0.06}$Dy$_y$Fe$_{2-y}$O$_4$ (y=0.00).

3.2.X ray diffraction (XRD)

X-ray diffraction (XRD) patterns of synthesized $Ni_{0.4}Co_{0.6}Dy_yFe_{2-y}O_4$ (y = 0.0, 0.03, 0.06, 0.09, 0.12 and 0.15) nano-ferrites were recorded at room temperature in the two theta range 10-70 $^{\circ}$. Fig. 2 depicts the XRD patterns of all compositions of $Ni_{0.4}Co_{0.6}Dy_yFe_{2-y}O_4$.The main reflection peaks were appeared at two theta values 30.24°, 35.66°, 43.30°, 47.29°, 54.22°, 57.50° and 62.20°. All these peaks correspond to hkl values (220), (311), (400), (331), (422), (511) and (440) respectively. These peaks were matched with standard data card ICSD:003-0875 ($NiFe_2O_4$).It is clear from the Figure, that when the concentration of the dopant Dy^{3+} was increased, an extra phase was appeared. The peaks of second phase are marked as *. This second phase identified as of Fe_2O_3. The peaks of Fe_2O_3 (a second phase) were matched with standard data card ICSD: 001-1053. The appearance of second phase may be due increased Dy contents.

Further the presence of major XRD peaks at similar (not identical) positions confirmed the successful substitution of rare earth Dy^{3+} cations in place of Fe^{3+}. From the Fig. 2, it is noted that the peak broadening takes place. This broadening is due to the involvement of f-orbitals which are deeply buried and give broad peaks in place of d-orbital which are exposed off and give sharp

peaks when Dy^{3+}ion replaces Fe^{3+} ion. The crystallite size was calculated by Debye Scherer's equation [20].

$$D = \frac{K\lambda}{\beta \cos\theta} \tag{1}$$

In above equation 1, D is crystallite size, λ is wavelength of X-rays, K is constant and has value 0.9 value, β is full width at half maximum of peaks and θ is Bragg's angle.

The values of crystallite size calculated from the equation (1) are given in Table 1 and are found in the range of 25-40 nm. The lattice parameter was calculated from the XRD data using following mathematical equation:

$$\frac{1}{d^2} = \frac{h^2 + k^2 + l^2}{a^2} \tag{2}$$

Here 'd' is interplaner distance; 'a' is cell length. The cell length calculated was 8.3488 Angstrom. The cell volume was 581.9277 $Å^3$.
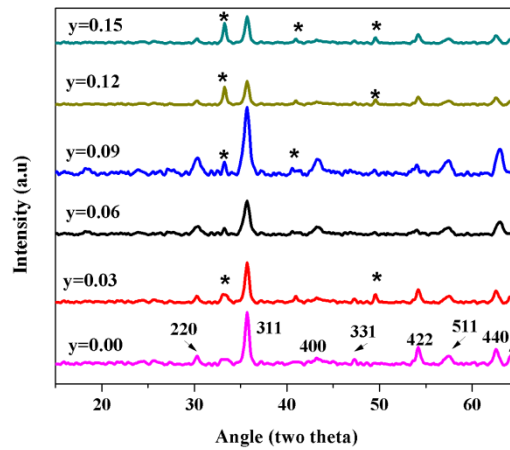

Fig. 2. XRD patterns of $Ni_{0.4}Co_{0.06}Dy_yFe_{2-y}O_4$ (y= 0.00, 0.03, 0.06, 0.09, 0.12 and 0.15) nanoparticles.

3.3.Fourier transform infrared (FTIR)analysis

Fig. 3 shows the fourier transform infrared (FT-IR) spectra of $Ni_{0.4}Co_{0.6}Dy_yFe_{2-y}O_4$ (y = 0.0, 0.06and 0.15) nano-ferrites. FTIR studies are important in predicting the position of ions in the crystal. There are two major absorption bands in the region of vibrational frequencies of 400-800 cm^{-1} i.e.,from 500-600 cm^{-1} for bending vibrations of iron-oxygen bond in tetrahedral complexes and from 350-500 cm^{-1} for stretching vibrations of iron-oxygen bond in octahedral complexes[21-23]. In the spectrum of un-doped nano-ferrite ($Ni_{0.4}Co_{0.6}Fe_2O_4$), there is a band at 555.50 cm^{-1} in tetrahedral region and a band at 430.13 cm^{-1} in octahedral region. In the spectrum of un-doped nanoferrite ($Ni_{0.4}Co_{0.6}Dy_{0.06}Fe_{1.94}O_4$)there is a band at 572.86 cm^{-1} in tetrahedral region but two bands at 433.98 cm^{-1} and 470.63 cm^{-1} in octahedral region. Likewise in the spectrum of doped nano-ferrite ($Ni_{0.4}Co_{0.6}Dy_{0.15}Fe_{1.85}O_4$) there is a band at 576.72 cm^{-1} in tetrahedral region but three bands at 499.56 cm^{-1}, 484.13 cm^{-1} and 460.99 cm^{-1} in the octahedral region. The increase in the number of bands in octahedral region by increasing the concentration of Dy^{3+} ion shows the replacement of Fe^{3+} ions by Dy^{3+} ions at octahedral position.
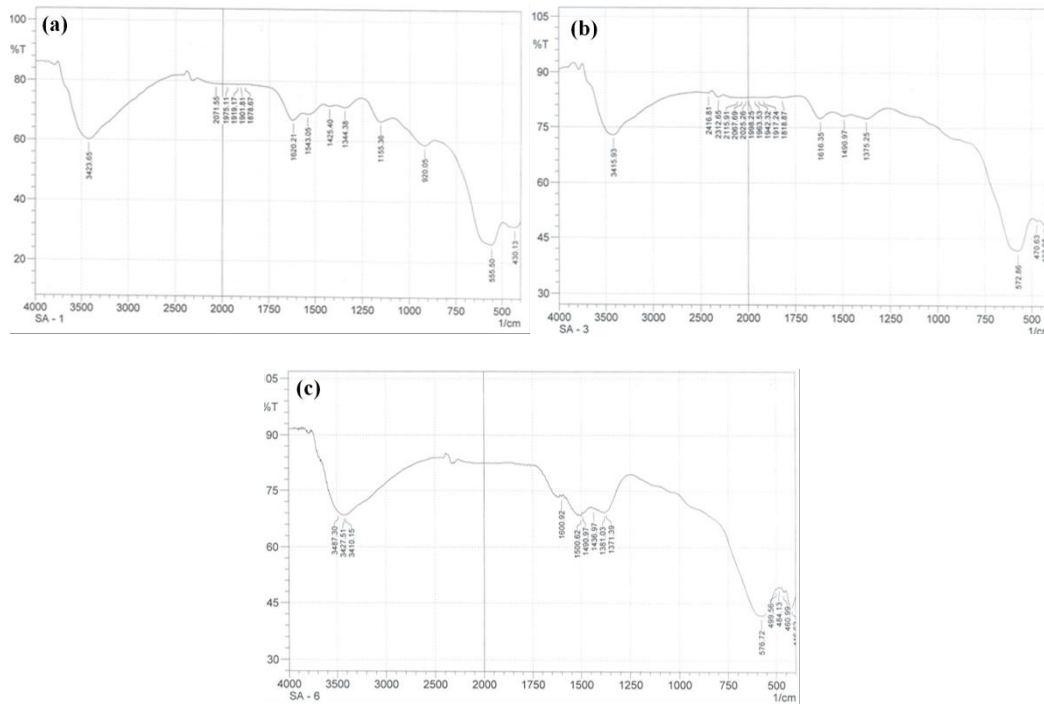
Fig. 3: FTIR spectra for $Ni_{0.4}Co_{0.06}Dy_yFe_{2-y}O_4$ (y= 0.00, 0.06 and 0.15) nanoparticles.

3.4. Dielectric measurements

Figs. 4, 5 and 6 show the effect of frequency of electric field on the dielectric constant (ε'), dielectric loss (ε'') and dielectric tanloss ($\tan\delta$) respectively. By applying electric field the material undergo polarization. This property is dielectric property which is also known as dielectric constant. The dielectric constant is due to the combination of two phenomena i.e. dipolar and interfacial polarization . Interfacial polarization is due to concentration of Fe^{+2} ions. By increasing frequency the concentration of Fe^{+2} ions decreases leading to the disappearance of interfacial polarization which results in overall decrease in dielectric constant. Dielectric constant can be calculated by the equation[24].

$$\varepsilon = \frac{cd}{\varepsilon_o A} \tag{3}$$

During the phenomenon of polarization, the atoms of material collide leading to the loss of electromagnetic radiations in the form of heat which is known as dielectric loss. Dielectric loss decreases by increasing frequency. Alternating current is applied leading to polarization and unpolarization of material. As the frequency increases this polarization and unpolarization doesn't match with the alternating current leading to decrease in polarization and in turn decrease in dielectric loss and dielectric tanloss which is the angle of dielectric loss This phenomenon is well explained by Maxwell-Wagner type interfacial polarization along with Koop's phenomenological theory[23, 25]. All the studied dielectric parameters (ε', ε'' and $\tan\delta$) decrease by increasing frequency due to material dispersion which is a frequency dependent property of material.

The variation of ε', ε'' and $\tan\delta$ with concentration of doped Dy^{3+} ion is shown in insets of Figs. 4, 5 and 6 respectively. By increasing concentration of Dy^{3+} ion, the dielectric properties decrease. The reason of this behavior is the concentration of Fe^{3+} ion which decreases by increasing Dy^{3+} ion and in fact Fe^{3+} ion is responsible for the polarizing power of material. When Fe^{3+} ion concentration decreases the polarization also decreases leading to decrease in dielectric properties.
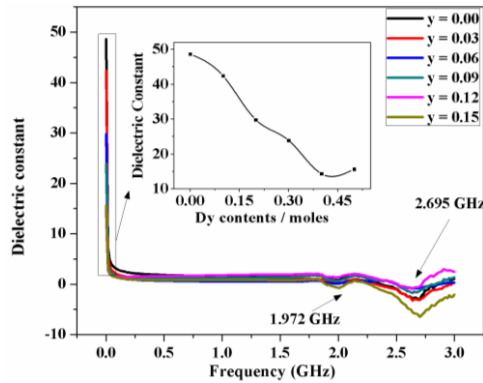
Fig. 4:Dielectric constant for Ni$_{0.4}$Co$_{0.06}$Dy$_y$Fe$_{2-y}$O$_4$(y= 0.00, 0.03, 0.06, 0.09, 0.12 and 0.15) nanoparticles
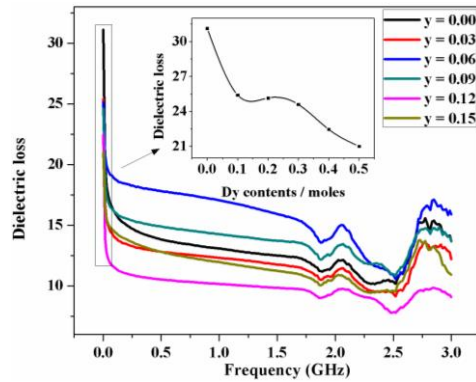

Fig. 5:Dielectric loss for Ni$_{0.4}$Co$_{0.06}$Dy$_y$Fe$_{2-y}$O$_4$(y= 0.00, 0.03, 0.06, 0.09, 0.12 and 0.15) nanoparticles
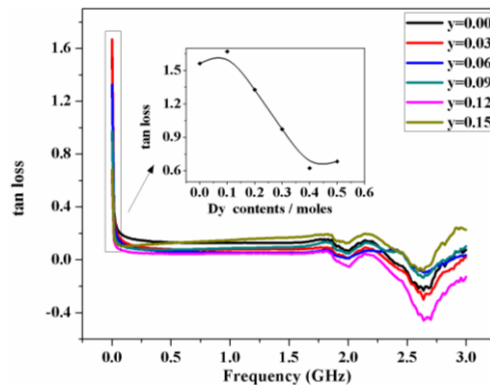

Fig. 6. tan loss for Ni$_{0.4}$Co$_{0.06}$Dy$_y$Fe$_{2-y}$O$_4$ (y= 0.00, 0.03, 0.06, 0.09, 0.12 and 0.15) nanoparticles

3.5.DC electrical resistivity

The temperature dependent DC electrical resistivity response of cobalt nickel nano-ferrites has been studied in the temperature range of 298 to 572 K by simple two probe method. DC electrical resistivity was calculated by the following equation.

$$\rho = \frac{RA}{d} \tag{4}$$

In above equation, the ρ is DC electrical resistivity, R is resistance, A is area and d is thickness of the pellet. The concentration dependence of room temperature DC electrical resistivity of all annealed cobalt nickel nano-ferrites is given in Table 1. It is evident from the data presented in Table 1 that by increasing Dy^{3+} ion concentration the value of ρ also increases. This is due to the incorporation of more resistive Dy^{3+} ion (92.6 x 10^{-8} Ω-m at 298 K) in place of less resistive Fe^{3+} ion (9.71×10^{8} Ω -m at 293K)[26].

The $\ln\rho$ vs. $10^{3}/T$ plots for all the annealed cobalt nickel nano-ferrites are presented in Fig. 7 and the values of regression coefficient for all the cobalt nickel ferrite samples reveal that the temperature dependent ρ data obey the following well known Arrhenius model .
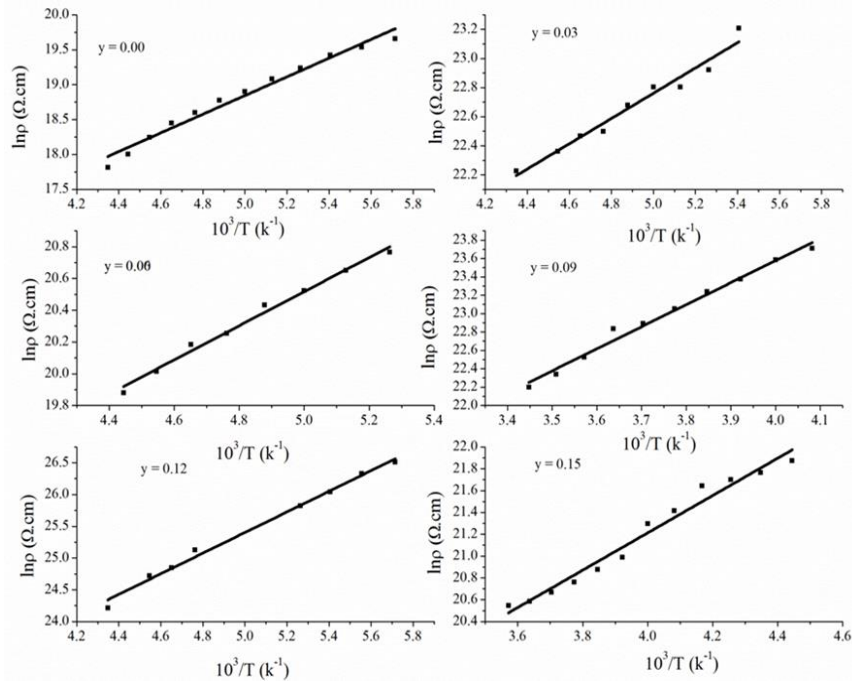

Fig. 7: Variation of lnρ with 10^{3}/T for $Ni_{0.4}Co_{0.06}Dy_yFe_{2-y}O_4$ (y= 0.00, 0.03, 0.06, 0.09, 0.12 and 0.15) nanoparticles.

$$\rho = \rho_o \exp\frac{\Delta E}{k_B T} \tag{5}$$

In above equation 5, the k_B is Boltzmann's constant, ΔE is energy of activation for hopping and ρ_0 is the resistivity when inverse of temperature approaches zero at x-axis. The behavior observed for DC electrical resistivity for these ferrites is such that it decreases by increasing temperature. This decreasing trend of DCelectrical resistivity with temperature shows that these ferrites are semiconductors. The reason of this behavior is that at higher temperature, these ferrites require very small amount of energy for the charge transfer and hence they have the high thermal mobility due to which by increasing temperature their thermal mobility also increases which results in decreased DC electrical resistivity.

The values of activation energy (ΔE_ρ) have been calculated by slope values of lnρ vs. $10^{3}/T$ plots (Figure 7) and are given in Table 1. The values of ΔE_ρ increase with concentration of Dy^{3+} ion and are due to the increase of DC electrical resistivity as discussed above.

Drift mobility

The drift mobility (μ_d) is an important parameter to study the charge transport properties of semiconductors and is given by the equation

$$\mu_d = \frac{1}{n_e \rho} \tag{6}$$

In above equation 6, the *n* is concentration of charge carriers and *e* is charge on electron. The value of *n* is further calculated by the equation 6, as given below.

$$n = \frac{N_A d_b P_{Fe}}{M} \tag{7}$$

In equation 7, the P_{Fe} is number of iron atoms, d is bulk density, N_A is Avagadro's number and M is molar mass of sample. The temperature dependence of drift mobility is given by the equation.

$$\mu_d = \mu_o \exp\left(\frac{-E_\mu}{k_B T}\right) \tag{8}$$

In this equation the k_B is Boltzmann constant, T is temperature, μ_0 is constant and E_μ is the activation energy. The temperature dependent drift mobility response is shown in $\ln\mu_d$ vs. $10^3/T$ plots (Figure 8). It has been observed that the drift mobility increases by increasing temperature. This can be explained on the basis of fact that drift mobility is inversely related to DC electrical resistivity and by increasing temperature charge carrier mobility increase which in turn increases the drift mobility.

The effect of concentration of Dy^{3+} ion on values of room temperature drift mobility is presented in Table 1and it has been found that drift mobility decreases by increasing Dy^{3+} ion contents. It is due to the incorporation of low mobility Dy^{3+} ion in place of relatively high mobility Fe^{3+} ion.

The values of activation energy (ΔE_μ) have also been calculated by the slope values of $\ln\mu_d$ vs. $10^3/T$ plots (Figure 8) and are listed in Table 1. Further, it has been observed that the values of ΔE_μ and ΔE_ρ are almost same.
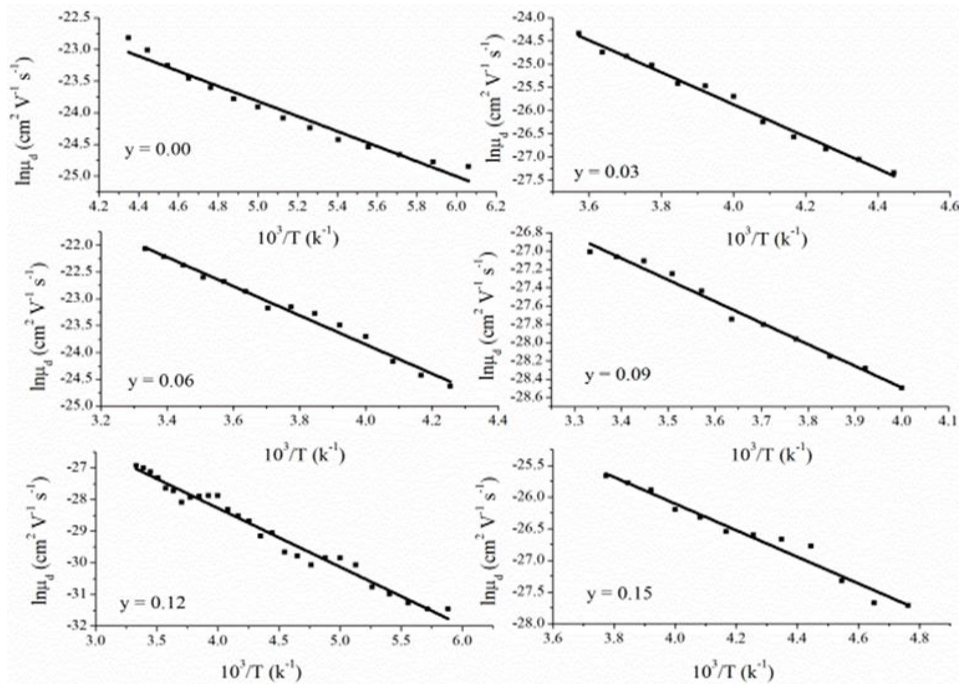

Fig. 8. Variation of $\ln\mu_d$ with $10^3/T$ for $Ni_{0.4}Co_{0.06}Dy_yFe_{2-y}O_4$ (y= 0.00, 0.03, 0.06, 0.09, 0.12 and 0.15) nanoparticles.

Table 1. Crystallite size (D), DC electrical resistivity (ρ at 298 K), drift mobility (μ_d at 298 K) and activation energies calculated from resistivity and drift mobility data (ΔE_ρ and ΔE_μ) of $Ni_{0.4}Co_{0.6}Dy_yFe_{2-y}O_4$ nanoferrites

Parameters	y = 0.0	y = 0.03	y = 0.06	y = 0.09	y = 0.12	y = 0.15
D (nm)	32	27	25	30	38	28
ρ (Ω.cm) (at 298 K)	$6.30 \times 10^{+08}$	$6.4 \times 10^{+08}$	$6.54 \times 10^{+08}$	$6.69 \times 10^{+08}$	$6.83 \times 10^{+08}$	$6.90 \times 10^{+08}$
ΔE_ρ (eV)	0.102	0.159	0.181	0.202	0.235	0.275
μ_d (cm^2 V^{-1} s^{-1}) (at 298 K)	1.49×10^{-11}	1.36×10^{-11}	1.31×10^{-11}	1.26×10^{-11}	1.1×10^{-11}	1.01×10^{-11}
ΔE_μ (eV)	0.103	0.159	0.182	0.204	0.234	0.272

4. Conclusions

Dysprosium substituted nickel cobalt nano-ferrites have been prepared by micro-emulsion method using CTAB as a surfactant. These ferrites were characterized by TGA, XRD, FTIR, DC electrical resistivity and dielectric measurements. XRD depicts that these ferrites are simple spinel having crystallite size in the range of 25 to 40 nm and they have face centered cubic structure. FTIR studies depict the presence of dysprosium metal ions which have replaced the iron ions.

Dielectric measurements showed the effect of varying frequency of electric field and concentration of dysprosium on the dielectric properties like dielectric constant, dielectric loss and dielectric tan loss and these properties decreased with increasing frequency of applied electric field. DC electrical resistivity increased while drift mobility decreased with increased dysprosium contents. Dielectric and DC electrical resistivity results suggest that these materials are the potential candidates for high frequency device applications.

Acknowledgement

References

[1] C.N.R. Rao, A.K. Cheetham, Science and technology of nanomaterials: Journal of Materials Chemistry**11**, 2887 (2001).
[2] M.F. Warsi, R.W. Adams, S.B. Duckett, V. Chechik, Chemical Communications **46,**451 (2010).
[3] K.M. Batoo, S. Kumar, C.G. Lee, Alimuddin, Current Applied Physics**9,**826 (2009).
[4] L.E. Smart, E.A. Moore, Solid State Chemistry: CRC Press **4th**, (2005).
[5] A. Sultan, A. Mahmood, N.K. Goraya, A.M. Qureshi, I. Ahmad, M.N. Ashiq, I. Shakir, M.F. Warsi, Journal of Alloys and Compounds **585,** 790 (2014).
[6] M.A. Nazir, M. Ul-Islam, I. Ali, H. Ali, B. Ahmad, S.M. Ramay, N. Raza, M.F. Ehsan, M.N. Ashiq, Journal of Elec Materi**45,** 1065 (2016).

[7] Valenzuela, R., Physics Research International, 2012 (2012).

[8] R. Ali, M.A. Khan, A. Mahmood, A.H. Chughtai, A. Sultan, M. Shahid, M. Ishaq, M.F. Warsi, Ceramics International**40,**3841 (2014).

[9] K.K. Bharathi, G. Markandeyulu, C.V. Ramana, The Journal of Physical Chemistry C **115**, 554 (2011).

[10] T. Zhou, D. Zhang, L. Jia, F. Bai, L. Jin, Y. Liao, T. Wen, C. Liu, H. Su, N. Jia, Z. Zheng, V.G. Harris, H. Zhang, Z. Zhong , The Journal of Physical Chemistry C **119,** 13207 (2015).

[11] Z. Peng, X. Fu, H. Ge, Z. Fu, C. Wang, L. Qi, H. Miao, Journal of Magnetism and Magnetic Materials**323**, 2513 (2011).

[12] M. George, S.S. Nair, A.M. John, P.A. Joy, M.R. Anantharaman, Journal of Physics D: Applied Physics**39,** 900 (2006).

[13] A. Mahmood, M.F. Warsi, M.N. Ashiq, M. Ishaq, Journal of Magnetism and Magnetic Materials **327,**64 (2013).

[14] A.K. Singh, A. Verma, O.P. Thakur, C. Prakash, T.C. Goel, R.G. Mendiratta, Materials Letters **57,** 1040 (2003).

[15] N. Guskos, J. Typek, G. Zolnierkiewicz, K. Wardal, D. Sibera, U. Narkiewicz, Reviews on Advanced Materials Science **129,** 142 (2011).

[16] C. Liu, B. Zou, A.J. Rondinone, Z.J. Zhang, The Journal of Physical Chemistry B **104,**1141 (2000).

[17] A. Mahmood, M. Nadeem, B. Bashir, I. Shakir, M.N. Ashiq, M. Ishaq, A. Jabbar, R. Parveen, M. Shahid, M.F. Warsi, Journal of Magnetism and Magnetic Materials **348,**82 (2013).

[18] Z. Anwar, M. Azhar Khan, A. Mahmood, M. Asghar, I. Shakir, M. Shahid, I. Bibi, M. Farooq Warsi, Journal of Magnetism and Magnetic Materials**355**, 169 (2014).

[19] M. Ejaz, A. Mahmood, M.A. Khan, A. Hussain, A. Sultan, A. Mahmood, A.H. Chughtai, M.N. Ashiq, M.F. Warsi, I. Shakir, Journal of Magnetism and Magnetic Materials **404**, 257 (2016).

[20] P. Debye, P. Scherrer, Physik. Z**17,**277 (1916).

[21] A.B. Salunkhe, V.M. Khot, M.R. Phadatare, N.D. Thorat, R.S. Joshi, H.M. Yadav, S.H. Pawar, Journal of Magnetism and Magnetic Materials**352**, 91 (2014).

[22] B. Zhou, Y.-W. Zhang, C.-S. Liao, C.-H. Yan, L.-Y. Chen, S.-Y. Wang, Journal of Magnetism and Magnetic Materials**280**, 327 (2004).

[23] D. Ravinder, Materials Letters**40,**205 (1999).

[24] M. Asif Iqbal, M.U. Islam, I. Ali, M.A. khan, I. Sadiq, I. Ali, Journal of Alloys and Compounds**586**, 404 (2014).

[25] C.G. Koops, Physical Review**83**, 121 (1951).

[26] S. Hussain, A. Maqsood, Journal of Alloys and Compounds**466**, 293(2008).